

# TRIPLE COVERINGS AND A GENUS-TWO SURFACE SPANNING AN ELONGATED TETRAHEDRON AND BEATING THE CONE

GIOVANNI BELLETTINI, MAURIZIO PAOLINI, AND FRANCO PASQUARELLI

ABSTRACT. Using a suitable triple covering space it is possible to model the construction of a minimal surface with genus two spanning all six edges of a tetrahedron, working in the space of BV functions and interpreting the film as the boundary of a Caccioppoli set in the covering space. The possibility of using covering spaces for minimal surfaces was first proposed by Brakke in [3], see also [1]. After a question raised by Bob Hardt in the late 1980's, it seems common opinion that an area-minimizing surface of this sort does not exist for a regular tetrahedron, although a proof of this fact is still missing. In this paper we show that there exists a surface of genus two spanning the boundary of an elongated tetrahedron and having area strictly less than the area of the conic surface.

## 1. INTRODUCTION

Finding a soap film that spans all six edges of a regular tetrahedron different from the classical conic minimal surface of Figure 1 (left) is an intriguing problem. It was discussed by Lawlor and Morgan in [8, p. 57, and fig. 1.1.1], where a sketch of a possible area-minimizing surface of genus two is shown, based on an idea of Bob Hardt<sup>1</sup>; such a surface is here reproduced in Figure 1 (right)<sup>2</sup>. The same picture was subsequently included in the book [10, fig. 11.3.2].

The cone constructed from the center of the solid spanning the six edges of the tetrahedron (Figure 1 left) has been proved to minimize area if one imposes on the competitors the extra constraint that they divide the regular tetrahedron in four regions, one per face [8]. It corresponds to the actual shape that a real soap film attains when dipping a tetrahedral frame in soapy water; it includes a  $T$ -singularity at the center, where four triple lines ( $Y$ -singularities) converge from the four vertices satisfying the local constraints of an area-minimizing surface [11].

---

DIPARTIMENTO DI INGEGNERIA DELL'INFORMAZIONE E SCIENZE MATEMATICHE, UNIVERSITÀ DI SIENA, 53100 SIENA, ITALY, AND INTERNATIONAL CENTRE FOR THEORETICAL PHYSICS ICTP, MATHEMATICS SECTION, 34151 TRIESTE, ITALY

DIPARTIMENTO DI MATEMATICA E FISICA, UNIVERSITÀ CATTOLICA DEL SACRO CUORE, 25121 BRESCIA, ITALY

DIPARTIMENTO DI MATEMATICA E FISICA, UNIVERSITÀ CATTOLICA DEL SACRO CUORE, 25121 BRESCIA, ITALY

*E-mail addresses:* [bellettini@diism.unisi.it](mailto:bellettini@diism.unisi.it), [maurizio.paolini@unicatt.it](mailto:maurizio.paolini@unicatt.it), [franco.pasquarelli@unicatt.it](mailto:franco.pasquarelli@unicatt.it).

*Date:* May 25, 2022.

<sup>1</sup> A sketch of this surface was found by F. Morgan in B. Hardt's office during a visit at Stanford around 1988. F. Morgan and J. Taylor tried to find crude estimates to compare the two minimizers without success. Many years later Hardt himself told R. Huff about the problem, who then came out with the results that can be found in [7].

<sup>2</sup> The picture itself is a computer generated image obtained by J. Taylor using the **surface evolver** of K. Brakke.

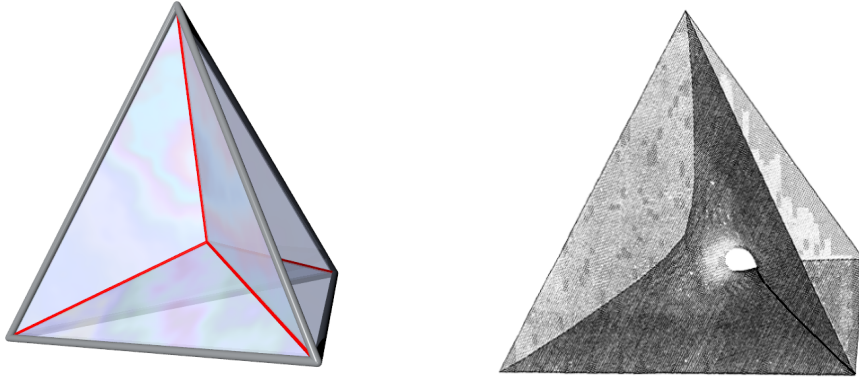


FIGURE 1. Left: the classic conical minimal film spanning a regular tetrahedron. Right: a slightly retouched version of [8, fig. 1.1.1]. In turn it is an enhanced version of [10, fig. 11.3.2]. Each triple curve “passes through” one of the two holes.

However, it is an open question whether a film with positive genus, e.g. with holes connecting pairs of faces, could beat the conelike configuration; Figure 1 (right) shows a theoretically feasible configuration of such a minimizing film.

Although it seems a common opinion, based both on physical experiments and theoretical reasons, that such a surface does not actually exist (see e.g. [7]), to our best knowledge such a question still remains open.

Generalizations of the problem, for instance considering deformations of the tetrahedron with the addition of zig-zags [7], allows on the contrary to construct a surface with the required topology that at least satisfies all local properties of a minimal film. Another generalization that could lead to interesting minimizers consists in considering anisotropic surface energies [8].

The surface of genus two depicted in Figure 1 includes two triple curves (curves where three sheets of the surface meet at  $120^\circ$  degrees) and no quadruple point. Furthermore it sports two “holes”, one clearly visible that allows to traverse the regular tetrahedron entering from the front face and exiting from the back. The other hole is located on the other side of the film and allows to traverse the tetrahedron entering from the right lateral face and exiting from the bottom face (without crossing the soap film). Figure 10 in Section 6 helps to realize the presence of the two holes.

Our first result (Section 4) is the construction of a covering space of degree 3 of the complement of the one-skeleton of a tetrahedron, following the lines of [3] (see also [1]), that is compatible with Figure 1, right. Using covering spaces allows to treat in a neat way situations that seem hard to model using other approaches. A small portion of the soap film somehow behaves like a sort of “portal” to a parallel (liquid) universe. More precisely, each point in  $\mathbb{R}^3$  (after removal of a suitable set of curves, obtaining the so-called base space) has two other counterparts, for a total of three copies of the base space that are actually to be interpreted (locally) as three distinct sheets of a covering. Globally the picture is more interesting, since the covering space is constructed in such a way that when travelling along a closed curve in the base space, the “lifted” point might find itself on a different sheet of the same fiber. This can be used as a trick to overcome the problem in treating the soap film as a transition layer between air and liquid leading to the superposition of two layers, since the water part has infinitesimal thickness. An approach based e.g. on  $BV$  functions would then miss completely the two superposed layers. Using

the covering space overcomes the problem by adding a “fake” big set of liquid fase, lying in a different sheet of the same fiber with an entry point corresponding to one face of the soap film and an exit point (reached travelling along suitable closed curves in the base space) from the other face of the soap film in the same position. A phase parameter  $u$  defined in the covering space is then defined with values in  $\{0, 1\}$ , 0 indicating liquid, 1 indicating air, in such a way that in exactly one of the three points of a fiber we have  $u = 1$  (air). Looping around an edge of the tetrahedron would take from one point to another of the same fiber, thus forcing the value of  $u$  to jump somewhere along the loop, which in turn would force the soap film to “wet” the edge.

The presence of triple curves implies that at least three sheets are required for a covering modelling the film problem, however the natural construction using suitable cyclic permutations of the three sheets when circling around each of the six edges of the regular tetrahedron cannot produce a surface with holes. This is because any path that traverses a tetrahedron entering from any face and exiting through another is by topological reasons linked to exactly one of the edges and hence forced to traverse the film. Some way to distinguish tight loops around an edge and loops that encircle the edge far away is then required.

The construction is then more involved and requires the introduction of two “invisible wires”. This is done in the same manner and for similar reasons as in [3, Section 5.1], see in particular examples 7.7 and 7.8 in that paper. After constructing the covering space, we can adapt the machinery of [1] (see Section 5), and settle the Plateau problem in  $BV$ , with the difference that the involved functions defined on  $Y$ , instead of taking values in an equilateral triangle (with the constraint of having zero sum on each fiber), take here values in  $\{0, 1\}$ , with the constraint indicated in (5.2).

Our next main result (Theorem 6.1) is to prove that, for a sufficiently elongated tetrahedron, there is a surface spanning its boundary, having the topology of the surface of Figure 1 right, and having area *strictly less* than the area of the conelike surface. Therefore, if we allow for competitors of higher genus, we expect the conelike surface not to be a solution of the Plateau problem. We remark that our result does not cover the case of a *regular* tetrahedron.

Positioning the invisible wires is delicate. We would like them not to influence the area-minimizing film, which requires that the minimizing film does not wet them. This is not proved here, although the numerical simulations strongly support this fact for a sufficiently elongated tetrahedron and suitably positioned invisible wires. On the other hand, the observations made in Section 7 show that a nonwetting relative area-minimizer does not exclude the existence of an absolute minimizer with the structure of Figure 14 which we would like to exclude. Again, the numerical simulations support the conjecture that if the invisible wires are positioned sufficiently far away from the short edges, then the absolute minimizer has the required topology (and does not wet the invisible wires). On the contrary, positioning the invisible wires near the short edges would produce wetting absolute minimizers.

## 2. THE BASE SPACE

In view of the symmetry<sup>3</sup> of the desired surface, it is convenient to think of the tetrahedron as a wedge with two short edges,  $S_1$  and  $S_2$ , and four long edges,  $L_i$ ,  $i = 1, \dots, 4$ ; for simplicity we name the union of all edges as  $S = (\cup_{i=1}^2 S_i) \cup (\cup_{i=1}^4 L_i)$ . A sketch of such a wedge is displayed in Figure 2.

---

<sup>3</sup>The symmetry group of the soap film of Figure 1 turns out to be  $\mathbb{D}_{2d}$ , using Schoenflies notation.

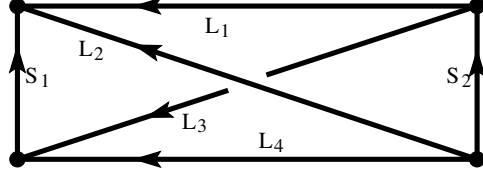


FIGURE 2. In view of the symmetry  $\mathbb{D}_{2d}$  of the desired surface, it is convenient to think of the tetrahedron as a wedge with two short edges,  $S_1$  and  $S_2$ , and four long edges,  $L_1, L_2, L_3, L_4$ . When required, the short edges are oriented upwards, the long edges are oriented from right to left.

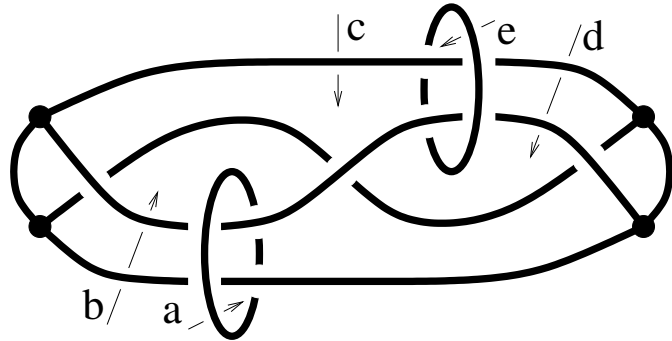


FIGURE 3. The base space  $M$  is  $\mathbb{R}^3$  with the displayed arcs removed. Arrows and labels correspond to the generators of a presentation of the fundamental group.

In order to construct a proper base space for our covering let us summarize the required properties of the soap film that we would like to obtain.

- (1) The soap film is required to wet all six edges of the tetrahedron/wedge. From the point of view of the covering space this is achieved by requiring that any path that circles once around an edge at a short distance acts on the fiber with no fixed point;
- (2) it is possible to find closed paths that suitably traverse the tetrahedron (with reference to Figure 1, one path entering from the front face and exiting from the back face, the other entering from the right face and exiting from the bottom face) that when lifted on the covering space do not move at least one point of the fiber.

The second requirement seems at first sight incompatible with the first one, since such traversing paths are actually forced to circle once around a single edge of the tetrahedron. This is unavoidable and a consequence of the topology of the graph having the six edges as arcs. However these paths are allowed to circle the edges “far away”, and we can make the two paths, the one circling (say) the edge on the left ( $S_1$  in Figure 2) at a short distance and the one traversing the visible hole in the soap film in Figure 1, not homotopically equivalent by introducing an obstruction in the base space in the form of an invisible wire. The invisible wire has the purpose of making the two paths not equivalent, but in the meantime we do not want it to “perturb” the soap film.

We actually need to introduce two invisible wires, in the form of two closed loops  $C_1, C_2$  suitably interlaced to the edges of the wedge. We name their union as  $C_{12} = C_1 \cup C_2$ . The result is illustrated in Figure 3, the base space  $M = \mathbb{R}^3 \setminus (S \cup C_{12})$

being the complement in  $\mathbb{R}^3$  of the system of curves displayed as thick lines. We shall use it to construct the covering space  $Y$ .

The picture follows the usual convention of inserting small gaps to denote *underpasses* of a curve below another. The four dots (vertices of the tetrahedron) represent points where three curves meet. This system of curves is the disjoint union of two loops ( $C_1$  and  $C_2$ ) and a set of two short curves ( $S_1, S_2$ ) and four long curves ( $L_1$  to  $L_4$ ) joining four points. The latter is topologically equivalent to the set of edges of a tetrahedron.

Each of the two  $C_1$  and  $C_2$  loops around a pair of long edges, they are called *invisible wires* in [3] and their presence is essential to allow for jump sets with the required topology. The loop  $C_1$  is the one nearest to the short edge  $S_1$ .

The quantity defined by the following definition plays an important role.

**Definition 2.1.** *Given a choice of the geometry of  $M$ ,  $\rho_\infty(M)$  is defined as the distance<sup>4</sup> from the two short edges and the invisible wires of  $M$ :*

$$\rho_\infty(M) := \min\{|x - y|_\infty : x \in S_1 \cup S_2, y \in C_1 \cup C_2\}.$$

*Remark 2.1.* In constructing the base space  $M$  we did not pay much emphasis on its geometry (see e.g. Figure 3), which is allowed as long as we study topological properties like its fundamental group, or when constructing the covering space  $Y$ .<sup>5</sup> However, when considering the minimal film, the actual geometry becomes important. We shall then make specific choices both for the set of curves corresponding to the tetrahedral frame, straight segments with two different lengths, and for the two closed curves corresponding to the invisible wires. We point out here that the two invisible wires can be safely deformed into straight lines, one in the  $y$  direction through  $(s, 0, 0)$ , the other in the  $z$  direction through  $(-s, 0, 0)$ , for a suitable choice of  $s > 0$ , observing that a straight line is a closed curve in the compactification  $\mathbb{S}^3$  of  $\mathbb{R}^3$ . To avoid problems at infinity, where the two invisible wires would intersect, we can deform one or both of them “far away” (outside the convex hull of  $S$ ).

**Definition 2.2.** *For two parameters  $h > 0$  and  $s \in (0, 1)$ , we define a specific geometry for  $M = M_{h,s}$  as follows. The four vertices of the wedge  $W$  are fixed at*

$$(h, \pm 1, 0), \quad (-h, 0, \pm 1), \quad (2.1)$$

*and connected with straight segments of length  $|S_1| = |S_2| = 2$ ,  $|L_i| = \sqrt{2 + 4h^2}$ ,  $i = 1, \dots, 4$ . The invisible wires are now selected as straight lines (possibly modified far away from  $W$ ),  $C_1 = \{(-sh, 0, t) : t \in \mathbb{R}\}$  and  $C_2 = \{(sh, t, 0) : t \in \mathbb{R}\}$ .*

Clearly, we have  $\rho_\infty(M_{h,s}) = h(1 - s)$ .

### 3. COMPUTING THE FUNDAMENTAL GROUP

We shall occasionally need to fix a base point  $m_0$  in  $M$ . It is positioned far away from the set of curves, its actual position is inessential and we shall think of it as the eye of the observer. Equivalently, we can position it at infinity after compactification of  $\mathbb{R}^3$  into  $\mathbb{S}^3$ .<sup>6</sup>

The fundamental group  $\pi_1(M)$  can be computed by using a technique similar to the construction of the Wirtinger presentation of a knot group. We position the

<sup>4</sup>The infinity norm  $\|x\|_\infty := \max(\|x_1\|, \|x_2\|, \|x_3\|)$  is used here for convenience in view of the estimates to follow.

<sup>5</sup>It should be noted here that the base space  $M$  must be path connected, locally path connected and semilocally simply-connected [5, Chapter 1.3].

<sup>6</sup>Since a single point into a three-space cannot obstruct a closed path, adding the point at infinity to  $\mathbb{R}^3$  does not impact the computation of the fundamental group, nor it will make any difference in the construction of the covering space. For that matter, it also makes no difference to substitute  $\mathbb{R}^3$  with a big ball compactly containing the tetrahedron.

base point  $m_0$  above the picture and select a small set of closed curves  $a, b, c, d, e$  that will serve as generators of the group. These curves (that represent elements of  $\pi_1(M)$ ) are displayed in Figure 3 as arrows to be interpreted as curves that start at  $m_0$  (the observer eye), run straight to the tail of one of the arrows, follow the arrow *below* one or two arcs of the system of curves and finally goes back straight to  $m_0$ .

In order to prove that the selected loops generate the whole fundamental group it is enough to construct curves that loop around each of the pieces of curves running from an underpass or node to another underpass or node.

As an example, the product  $c^{-1}d$  is equivalent to a curve that loops around the piece of intermediate edge running from one disk to the other ( $L_{2,2}$  in the notation fixed below). This can be seen by observing that the  $d$  loop can be dragged from the right to the left of the top-right circle.

At this point we can construct  $bc^{-1}d$  looping around the bottom-right piece of curve from the underpass to the lower-right node.

Curve  $c^{-1}b$  corresponds to one of the four arcs in which the long edge connecting the lower-left to the upper-right node is divided.

Traversing an underpass can be achieved by conjugation with the loop corresponding to the overpass, which allows to obtain all the curves associated to the long edges. Product of two of these finally allows to loop around the short edges on the left and on the right. We end up with the following table, where the second index denotes what piece of the long arc of the wedge we are referring to (from left to right):

$$\begin{aligned} L_{1,1} &\rightarrow c, & L_{1,2} &\rightarrow ece^{-1}, \\ L_{2,1} &\rightarrow ac^{-1}da^{-1}, & L_{2,2} &\rightarrow c^{-1}d, & L_{2,3} &\rightarrow ec^{-1}de^{-1}, \\ L_{3,2} &\rightarrow c^{-1}b, & L_{3,3} &\rightarrow d^{-1}bc^{-1}d, \\ L_{4,1} &\rightarrow ad^{-1}cb^{-1}a^{-1}, & L_{4,2} &\rightarrow d^{-1}cb^{-1}, \\ S_1 &\rightarrow ad^{-1}ca^{-1}c^{-1}, & S_2 &\rightarrow bc^{-1}ece^{-1}. \end{aligned} \tag{3.1}$$

We omit the values associated to  $L_{3,1}$  and  $L_{3,4}$  (readily deducible by conjugation due to traversal of, respectively,  $L_{2,1}$  and  $L_{2,3}$ ), since we shall not need them.

Each crossing provides a relation among the three curves involved. By collecting all such relations and simplifying we finally end up with the presentation (five generators and two relators)<sup>7</sup>

$$\pi_1(M) = \langle a, b, c, d, e; ab = ba, de = ed \rangle \tag{3.2}$$

A different and more direct way to obtain the presentation (3.2) consists in an ambient deformation of (a tubular neighborhood) of the set of curves of Figure 3. An important remark here is that it is possible to flip the configuration of a “Steiner-like” pair of adjacent triple junctions as shown in Figure 4 without changing the homotopy type of both the set of curves and of its complement in  $\mathbb{R}^3$ . This allows to transform the set of curves of Figure 3 by homotopy equivalence into the first configuration of Figure 5. Then we shrink two curves to a point in the passage from the second to the third configuration, and again one curve from the third to the last without modifications to the homotopy type of both the set of curves and of its complement in  $\mathbb{R}^3$ .

Using this equivalence we can deform the set of curves as shown in Figure 5 to a bouquet of three loops with two linked rings, a configuration consistent with the presentation (3.2) for the fundamental group of the complement.

---

<sup>7</sup>This is actually a right-angled Artin group.

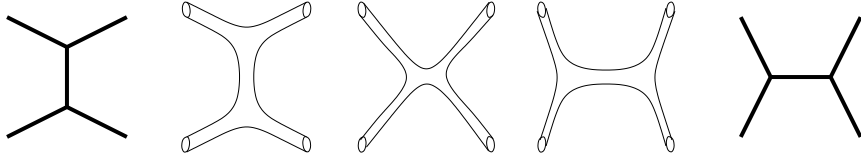


FIGURE 4. A tubular neighborhood of the Steiner tree on the left can be ambiently deformed into a tubular neighborhood of the Steiner tree on the right.

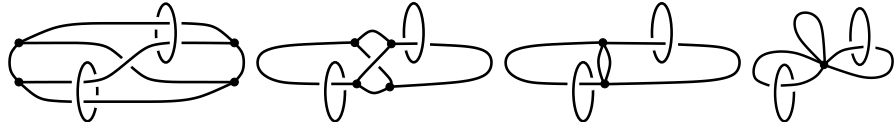


FIGURE 5. A sequence of steps showing that a tubular neighborhood of the system of curves can be ambiently deformed into a (tubular neighborhood of a) bouquet of three loops with two linked rings.

It should be noted that the graphs in the sequence of Figure 5 are not mutually homeomorphic, nor they are homeomorphic to the system of curves of Figure 3, whereas their complement in  $\mathbb{R}^3$  is diffeomorphic. We have an ambient isotopy as soon as we substitute each system of curves with a small tubular neighbourhood.

#### 4. THE COVERING SPACE

The presence of triple lines in the soap film that we would like to reconstruct (Figure 1, right) implies that the covering space must be at least of degree three. There is no quadruple (tetrahedral) point in this film, so that three sheets for the covering might be sufficient.

However, the particular structure of the surface (a single smooth component of the film that arrives to a triple line from two distinct directions) requires special treatment, similar to that of Examples 7.7 and 7.8 of [3], with the introduction of the so-called *invisible wires*. These are introduced as two copies of  $\mathbb{S}^1$  having the purpose of exchanging sheets 2 and 3, whereas sheet 1 is glued to itself.

As we shall see in Section 8 the introduction of the invisible wires is essential, in the sense that a covering with three (or two) sheets of the complement of the six tetrahedral edges is incompatible with the wetting conditions imposed on all edges.

A *cut and paste* construction of our covering is as follows [1].

- Take three copies of the base space  $M$  (complement in  $\mathbb{R}^3$  of the system of curves shown in Figure 3): sheet 1, 2 and 3;
- cut them along the shaded surfaces<sup>8</sup> displayed in Figure 6;
- Glue the three sheets again in such a way that when crossing the large surface cut the three sheets are glued cyclically. When crossing the shaded disks sheets 2 and 3 get exchanged whereas sheet 1 on one side is glued to sheet 1 on the other side.

*Remark 4.1* (Cutting locus as a stratified set). The set of cutting surfaces of Figure 6 forms a stratification composed by seven pieces of (2D) smooth surfaces joined by

<sup>8</sup>The set of shaded surfaces and the system of curves give rise to a stratification where the two-dimensional stratum (the cutting surfaces) is divided into connected components. The gluing permutation locally associated to each component can be transported along the whole component and must close consistently along closed paths on the surface. This would be a problem for non-orientable components (which is not our case) unless the permutation is of order two. In particular this is not an issue for coverings of degree 2.

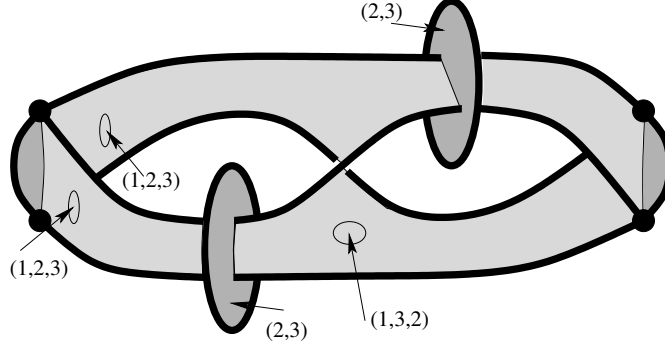


FIGURE 6. The covering is defined by a cut and paste technique on three copies of the base space cutted along the shaded surfaces. Local orientation is indicated, as well as the gluing among the sheets, with cycle notation.

four (1D) arcs (thin arcs in the picture, two triple curves and two selfintersection curves) and four (0D) end-points of the two selfintersection curves. The stratification as a whole is bounded by the set of curves defining  $M$  (thick curves in the picture) and by the four vertices of  $W$ . Each piece of 2D surface is orientable, and a choice of orientation is indicated by arrows, with one exception: the two small lunette-like dark regions on the left and on the right, which are oriented from front to back (however they are not a critic part of the cutting locus, see Remark 4.2). It should be noted that the large piece of surface connecting the two disks is subjected to a twist in the region near the center of the picture, so that the two corresponding arrows are oriented opposite to each other. One of them, say the one in the back (left in the picture), points in the opposite direction with respect to the chosen orientation, which is consistent with the associated inverse (cyclic) permutation. The gluing is based on the permutations shown in the picture (expressed in cycle notation) when crossing the surface in the direction of the arrows. The two intersection curves between the disks and the other surfaces impose a constraint upon the permutations on the left and on the right, which must be related by a conjugation defined by the transposition  $(2, 3)$  associated to both disks. This is a consequence of the exchange of sheets 2 and 3 performed across the disks. On the lunette surface to the left the permutation is  $(1, 3, 2)$  when crossing from front to back. It cannot be chosen arbitrarily and has to be the product of the nearby  $(1, 2, 3)$  permutations. Similarly, the permutation associated to the right lunette is forcibly given by  $(1, 2, 3)$ .

We denote by  $p : Y \rightarrow M$  the covering defined in this way.

*Remark 4.2.* It is not actually necessary to use triple lines in the covering definition. The two left and right small fins could be removed and the two sides of the large surface could be extended up to the short lateral edges of the tetrahedral wedge. The chosen cut surface just mimics the structure that we expect for the minimizing film.

**4.1. The covering is not normal.** The covering  $p : Y \rightarrow M$  is clearly path connected. We claim that it is not normal [5, Chapter 1.3], as a consequence of the fact that sheet 1 is somehow specially treated by the gluing performed at the two

disks. We recall that a covering is normal if for any pair  $x, y \in Y$  with  $p(x) = p(y)$  there exists a deck transformation<sup>9</sup>  $\psi : Y \rightarrow Y$  with  $\psi(x) = y$ .

**Proposition 4.1.** *The covering  $p : Y \rightarrow M$  is not normal.*

*Proof.* It is sufficient to show that the identify is the only deck transformation. Suppose by contradiction that  $\psi$  is a nontrivial deck transformation. Then  $\psi$  has no fixed points [5, page 70]. Now take  $x \in p^{-1}(m_0)$  in sheet 1,  $m_0$  being the base point of  $\pi_1(M)$ . Then  $\psi(x) = y$  belongs to either sheet 2 or 3; suppose for definiteness that it belongs to sheet 2. If  $\gamma$  is a closed path in  $M$  corresponding to  $a$  (Fig. 3) of  $\pi_1(M)$ , we can lift  $\gamma$  to  $Y$  into two distinct paths, one starting at  $x$ , the other starting at  $y$ . These paths are mapped into each other by the homeomorphism  $\psi$ , however one is closed (the one starting at  $x$ ), whereas the other is open, since when traversing the disk, the lifted path will continue on sheet 3. This gives a contradiction.  $\square$

**4.2. Abstract definition of the covering.** It is well known that an abstract definition of a covering of  $M$  is based on selecting a subgroup  $H$  of  $\pi_1(M)$ , considering the set  $\hat{Y}$  of paths  $\gamma : [0, 1] \rightarrow M$  with  $\gamma(0) = m_0$  and taking the quotient with respect to the equivalence relation

$$\gamma_1 \sim \gamma_2 \iff \gamma_1(1) = \gamma_2(1) \text{ and } [\gamma_1 \gamma_2^{-1}] \in H,$$

where  $\gamma_2^{-1}$  denotes the path  $\gamma_2$  with opposite orientation, and defining the projection as  $[\gamma] \rightarrow \gamma(1)$ . The degree of the covering is given by the index of  $H$  in  $\pi_1(M)$ . We shall then describe a procedure to produce a subgroup  $H$  of index 3 in  $\pi_1(M)$  (finitely presented in (3.2)) and subsequently prove in Theorem 4.3 that the procedure above produces a covering isomorphic to  $p : Y \rightarrow M$ .

In order to construct  $H$  we need a concrete way to identify its elements when written as words in the generators of the presentation (3.2). The first task is then to compute the actions  $\sigma_a, \sigma_b, \sigma_c, \sigma_d, \sigma_e$  on the fiber  $\{\hat{m}_0^1, \hat{m}_0^2, \hat{m}_0^3\}$  on the base point  $m_0 \in M$  (the superscripts refer to the three sheets 1, 2, 3), corresponding to each generator in (3.2). This amounts in associating to each generator the resulting permutation induced on sheets 1, 2, 3. A quick check comparing Figures 3 and 6 suggests then to define

$$\sigma_b = \sigma_d = (), \quad \sigma_a = \sigma_e = (2, 3), \quad \sigma_c = (1, 3, 2),$$

where  $()$  denotes the identity permutation. Observe that  $\sigma_a$  and  $\sigma_b$  commute, as well as  $\sigma_d$  with  $\sigma_e$ , so that the two relators in (3.2) are consistent with these actions. Given an element of  $\pi_1(M)$  expressed as a word  $w$  in the generators, by substituting these actions to the generators in  $w$  and performing the multiplications (left to right), we are then able to compute the action of the element represented by  $w$  on the fiber  $\{\hat{m}_0^1, \hat{m}_0^2, \hat{m}_0^3\}$  in terms of a permutation of the three superscripts.  $H$  will then be recovered as those words that produce a permutation fixing  $1 \in \{1, 2, 3\}$ . Using relations satisfied by the actions  $\sigma_a$  through  $\sigma_e$  we can simulate the final multiplication after substitution in  $w$  by imposing such relations directly on the generators, the result would be the same. So we can safely add such relations to the presentation (3.2) as extra relators<sup>10</sup>

$$K := \langle a, b, c, d, e; ab = ba, de = ed, b, d, e = a, a^2, c^3, ca = ac^2 \rangle$$

to obtain a new group  $K = \pi_1(M)/\hat{H}$  and a projection  $q : \pi_1(M) \rightarrow K$ , where  $\hat{H}$  is the normal subgroup of  $\pi_1(M)$  generated by the added relators. A sequence of

<sup>9</sup> A deck transformation is a homeomorphism  $\psi : Y \rightarrow Y$  such that  $p(\psi(x)) = p(x)$  for any  $x \in Y$ .

<sup>10</sup> The presence of  $a^2, c^3$  and  $ca = ac^2$  in the list of relators is due to the fact that  $\sigma_a^2 = \sigma_c^3 = ()$ , and  $\sigma_c \sigma_a = \sigma_a \sigma_c^2$ .

Tietze transformations [9] reduces the above presentation to  $K = \langle a, c; a^2, c^3, ca = ac^2 \rangle$  which is quickly seen to be isomorphic to the symmetric group  $S_3$  with representative elements  $\mathcal{S} := \{a^\alpha c^\gamma : \alpha \in \{0, 1\}, \gamma \in \{0, 1, 2\}\} \subset \pi_1(M)$ . Upon identification of the representative elements with their equivalence class, the projection  $q$  can be interpreted as a projection  $q : \pi_1(M) \rightarrow \mathcal{S}$ .

Finally, the subgroup  $H \leq \pi_1(M)$  is defined as the set of  $g \in \pi_1(M)$  such that  $\gamma = 0$  if we write  $q(g)$  as  $q(g) = a^\alpha c^\gamma \in \mathcal{S}$ . It corresponds to all paths in  $\pi_1(M)$  that remain closed when lifted on  $Y$  with starting point  $\hat{m}_0^{-1}$  taken in sheet 1.

As an example, consider the word  $w = ad^{-1}ca^{-1}c^{-1}$  (this word corresponds to looping once around the short edge  $S_1$ , (3.1)). We can remove all occurrences of  $b$  and  $d$  and substitute  $a$  for  $e$  to obtain the word  $aca^{-1}c^{-1}$ . Enforcing  $a^2 = c^3 = 1$  (empty word) we arrive at  $acac^2$ ; using  $ca = ac^2$  then produces  $a^2c^4$  that finally reduces to the normal form  $a^\alpha c^\gamma$ , with  $\alpha = 0, \gamma = 1$ . Since  $\gamma \neq 0$  we conclude that  $w \notin H$ .

**Proposition 4.2.** *The subgroup  $H$  has index 3 in  $\pi_1(M)$  and it is not a normal subgroup.*

*Proof.* That  $H$  is a subgroup is a direct check. Its right cosets are obtained by right multiplication by  $\gamma$  and  $\gamma^2$  showing that there are exactly three cosets (they correspond to  $\gamma = 0, 1, 2$  in  $\mathcal{S}$ ). It is not a normal subgroup since  $a \in H$  ( $a = a^1c^0$ , hence  $\gamma = 0$ ), but  $cac^{-1} \notin H$ . Indeed  $q(cac^{-1}) = q(ac)$  by enforcing  $ca = ac^2$ ). The non normality of  $H$  is consistent with the non normality of the covering.  $\square$

The next result ensures in particular that the approach of Section 5 is independent of the choice of the cut surface.

**Theorem 4.3.** *The covering defined by  $H \leq \pi_1(M)$  using the procedure above is isomorphic to the covering  $p : Y \rightarrow M$  defined with the cut and paste technique.*

*Proof.* The proof consists in a direct check that  $\pi_1(M)$  defines the same action on the fiber above the base point of  $M$  after identifying sheet 1 of the cut/paste construction with the equivalence class corresponding to the subgroup  $H$  in the abstract construction.  $\square$

**4.3. Structure of the branch curves.** The covering space  $Y$ , viewed as a metric space with the metric locally induced by the base space  $M$ , can be completed into  $\overline{Y}$  with the addition of *branch curves*. The projection  $p$  then naturally extends to

$$p : \overline{Y} \rightarrow \mathbb{R}^3$$

which will now be a branched covering.

Of particular importance are the branch curves corresponding to Cauchy sequences that converge in  $M$  to points belonging to the invisible loops  $C_1$  and  $C_2$ .

**Theorem 4.4.** *The inverse image  $p^{-1}(C_1)$  consists of two connected components,  $p^{-1}(C_1) = C_1^1 \cup C_1^{23}$ :  $C_1^1$  being a ramification curve of index one, i.e. having a small tubular neighborhood homeomorphic to its projection into a tubular neighborhood of  $C_1 \subset M$ ;  $C_1^{23}$  being a ramification curve of index two, with a small tubular neighborhood that projects onto its image as a branched covering of degree two. Similar properties hold for  $C_2$ .*

*Proof.* This is a direct consequence of cut and paste construction of the covering, in particular of the fact that the permutation of sheets associated to the two disks fixes sheet 1 and swaps sheets 2 and 3.  $\square$

## 5. THE MINIMIZATION PROBLEM

We refer to [2] for all details on functions of bounded variation; we denote by  $\mathcal{H}^\ell$  the  $\ell$ -dimensional Hausdorff measure in  $\mathbb{R}^3$ , for  $\ell = 1, 2$ .

For any specific (geometric) definition of  $M$  and  $Y$ , we set

$$D_0(\mathcal{F}) := \left\{ u \in BV(Y; \{0, 1\}) : \sum_{y \in p^{-1}(x)} u(y) = 1 \text{ for a.e. } x \in M \right\} \quad (5.1)$$

Then we impose a “Dirichlet” boundary condition at infinity, and the domain of the functional  $\mathcal{F}$  is defined as

$$D(\mathcal{F}) := \{u \in D_0(\mathcal{F}) : u(y) = 1 \text{ for a.e. } y \in \text{sheet 1 of } p^{-1}(x), |x| > C\} \quad (5.2)$$

for  $C$  large enough such that the ball of radius  $C$  compactly contains the solid wedge  $W$ . In view of the fact that the covering is not normal (Proposition 4.1), the choice of the Dirichlet condition is now quite important.

Finally, the functional to be minimized is

$$\mathcal{F}(u) = \begin{cases} \frac{1}{2}|Du|(Y) & \text{if } u \in D(\mathcal{F}), \\ +\infty & \text{otherwise.} \end{cases}$$

The presence of the constant  $1/2$  is due to the fact that, if  $u$  jumps at a point of a sheet, then the constraint in (5.2) forces  $u$  to jump also at the corresponding point (i.e., on the same fiber) of another sheet, while on the remaining sheet  $u$  does not jump.  $|Du|$  is the usual total variation for the scalar-valued function  $u$ .

Given  $u \in D_0(\mathcal{F})$ , we denote by  $J_u \subset Y$  the jump set of  $u$ .

**Definition 5.1.** *The “film surface” is defined as  $p(J_u) \subset M$ .*

The film surface behaves well with respect to the jump set, in the sense that the total variation has the following representation:

**Theorem 5.1.** *For all  $u \in D_0(\mathcal{F})$  we have  $\mathcal{H}^2(p(J_u)) = \mathcal{F}(u)$ .*

*Proof.* It is enough to repeat the arguments of [1, Lemma 2.12], by using local parametrizations of  $Y$ , and 2-rectifiability of the jump set of a  $BV$ -function.  $\square$

**Definition 5.2.** *For a given geometry  $M$  of the base space, the minimum value of  $\mathcal{F}$  depends on  $M$ ; we set*

$$\mathcal{F}_{\min}(M) := \inf_{u \in D(\mathcal{F})} \mathcal{F}(u).$$

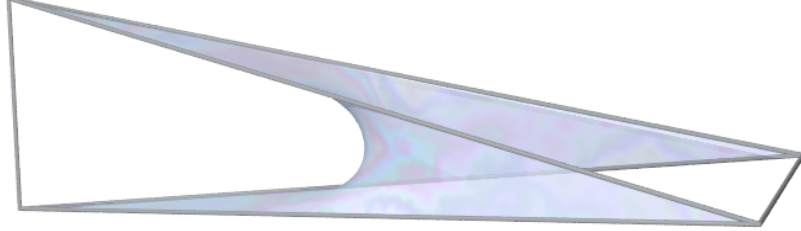
By the semicontinuity and compactness properties of  $\mathcal{F}$ , the infimum on the right hand side is actually a minimum [1].

**Theorem 5.2** (Wetting condition). *Given  $u \in D(\mathcal{F})$  the set  $p(J_u)$  satisfies the following properties:*

- (P1) *any closed curve that loops around a long edge  $L_1, L_2, L_3$  or  $L_4$  intersects  $p(J_u)$ ;*
- (P2) *any closed curve that loops around a short edge  $S_1$  or  $S_2$  at a distance smaller than  $\rho_\infty(M)$  intersects  $p(J_u)$ .*

*In particular, it is possible that a closed curve around  $S_1$  or  $S_2$  does not intersect  $p(J_u)$ .*

By “loops around an edge” we mean that it can be continuously deformed without crossing any edge of the tetrahedron into a “meridian” of the edge, a loop that orbits around that edge alone at a small distance.

FIGURE 7. The minimal film spanning the long edges of  $W$  ( $h = 3.5$ ).

*Proof.* Let  $x \notin p(J_u)$  and take the precise representative of  $u$  (still denoted by  $u$ ). By construction of the covering space a loop<sup>11</sup> in  $M$  based at  $x$  around anyone of the long edges lifts into a path that moves all sheets of the fiber on  $x$ , in particular it moves the fiber where  $u = 1$  taking it into a fiber where  $u = 0$  (condition in (5.1)). This forces  $u$  to jump along the loop. This gives (P1). Property (P2) is proved similarly by observing that a curve that loops around, say  $S_1$  at a distance smaller than  $\rho_\infty(M)$  cannot also interlace  $C_1$  and again when lifted in the covering space it moves all points of the fiber.  $\square$

**5.1. Estimate of  $\mathcal{F}_{\min}(M)$  from below.** A crude estimate from below of  $\mathcal{F}_{\min}(M)$  is a direct consequence of property (P1) above, indeed property (P1) is also satisfied by the area-minimizing surface  $\Sigma_{\text{skew}}$  that spans the skew quadrilateral defined by the long edges  $L_i$ ,  $i = 1, 2, 3, 4$  (Figure 7).

*Remark 5.1.* We have

$$2h \leq \mathcal{H}^2(\Sigma_{\text{skew}}) \leq \sqrt{4h^2 + 1} + 1. \quad (5.3)$$

The lower bound can be obtained by reasoning as in Theorem 5.3 below, whereas the upper bound is the area of the surface obtained by taking the upper and lower faces of  $W$  for  $x < 0$ , the central (unit) square  $W \cap \{x = 0\}$  and the front and back faces for  $x > 0$ .

Set  $M = M_{h,s}$  for a given choice of  $h$  and  $s$ . For any given  $u \in D(\mathcal{F})$ , the projection  $p(J_u)$  of the jump set of  $u$  satisfies properties (P1) and (P2) of Theorem 5.2. This allows us to obtain an estimate from below of its  $\mathcal{H}^2$  measure.

For  $t \in [-1, 1]$  take the plane  $\pi_t = \{x = ht\}$ . Its intersection  $R$  with the wedge  $W$  is a rectangle of sides  $1+t$  and  $1-t$ . We shall derive an estimate from below of  $\mathcal{H}^1(p(J_u) \cap \pi_t)$ .

**5.1.1. Case  $|t| > s$ .** We have  $\rho_\infty(M) = h(1-s)$  so that the  $L^\infty$ -distance of  $\pi_t$  from  $S_2$  if  $t > 0$  (resp.  $S_1$  if  $t < 0$ ) is less than  $\rho_\infty(M)$ . As a consequence any curve in the rectangle  $R$  that connects its two long sides can be closed as a loop around  $S_2$  (resp.  $S_1$ ) at an  $L^\infty$ -distance smaller than  $\rho_\infty(M)$  and in view of (P2) of Theorem 5.2 is forced to intersect  $p(J_u) \cap \pi_t$ . This, together with the first property, is enough to conclude that the size of  $p(J_u) \cap \pi_t$  cannot be less than both the size of the Steiner tree joining the four vertices of  $R$  and twice the length of the long sides of  $R$ . Hence

$$\mathcal{H}^1(p(J_u) \cap \pi_t) \geq \min\{1 + \sqrt{3} - (\sqrt{3} - 1)|t|, 2 + 2|t|\}.$$

<sup>11</sup> To get an element of  $\pi_1(M)$  we need to select a path from  $m_0$  to any point of the loop. The element of  $\pi_1(M)$  consists in first moving along such path, then following the loop and finally going backwards to  $m_0$  along the selected path. This does not impact the reasoning above.

Comparing the two arguments of the minimum this inequality splits in two cases

$$\mathcal{H}^1(p(J_u) \cap \pi_t) \geq \begin{cases} 2 + 2|t| & \text{if } |t| < 2 - \sqrt{3}, \\ 1 + \sqrt{3} - (\sqrt{3} - 1)|t| & \text{if } |t| \geq 2 - \sqrt{3}. \end{cases} \quad (5.4)$$

5.1.2. *Case  $|t| \leq s$ .* We can still enforce (P1) of Theorem 5.2: any curve in  $R$  connecting two adjacent sides can be completed into a loop around one of the long edges  $L_i$ ,  $i \in \{1, 2, 3, 4\}$  and hence it must intersect  $p(J_u) \cap \pi_t$ . It follows that the size of  $p(J_u) \cap \pi_t$  cannot be less than twice the length of the short sides of  $R$

$$\mathcal{H}^1(p(J_u) \cap \pi_t) \geq 2 - 2t. \quad (5.5)$$

**Theorem 5.3.** *For a given choice of  $h$  and  $s$ , we have:*

$$\mathcal{F}_{min}(M_{h,s}) \geq \begin{cases} 2h(4 - \sqrt{3} - 2s^2) & \text{if } s < 2 - \sqrt{3}, \\ h[3 + \sqrt{3} - 2(\sqrt{3} - 1)s - (3 - \sqrt{3})s^2] & \text{if } s \geq 2 - \sqrt{3}. \end{cases} \quad (5.6)$$

*Proof.* *Case  $s < 2 - \sqrt{3}$ .* Using the generalized coarea formula [4, Theorem 3, pag. 103] and the sectional estimates (5.4) and (5.5), we have

$$\begin{aligned} \mathcal{H}^2(p(J_u)) &\geq \int_{-h}^h \mathcal{H}^1(p(J_u) \cap \pi_t) dt \\ &\geq 2h \int_0^s (2 - 2t) dt \\ &\quad + 2h \int_s^{2-\sqrt{3}} (2 + 2t) dt \\ &\quad + 2h \int_{2-\sqrt{3}}^1 \left[ 1 + \sqrt{3} - (\sqrt{3} - 1)t \right] dt \\ &= 2h[(2s - s^2) + (11 - 6\sqrt{3} - s^2 - 2s) + (5\sqrt{3} - 7)] \\ &= 2h(4 - \sqrt{3} - 2s^2). \end{aligned}$$

*Case  $s \geq 2 - \sqrt{3}$ .* The intermediate integral now disappears. We get

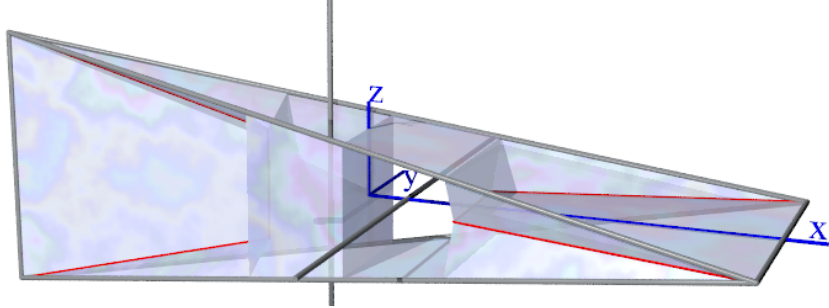
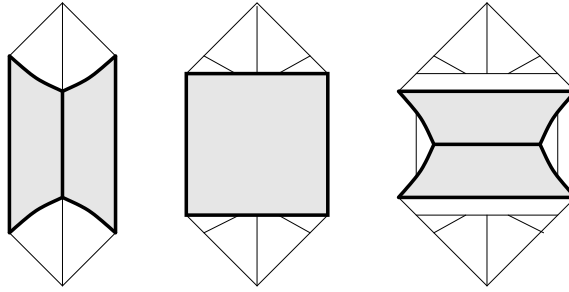
$$\begin{aligned} \mathcal{H}^2(p(J_u)) &\geq \int_{-h}^h \mathcal{H}^1(p(J_u) \cap \pi_t) dt \\ &\geq 2h \int_0^s (2 - 2t) dt \\ &\quad + 2h \int_s^1 \left[ 1 + \sqrt{3} - (\sqrt{3} - 1)t \right] dt \\ &= h[3 + \sqrt{3} - 2(\sqrt{3} - 1)s - (3 - \sqrt{3})s^2]. \end{aligned}$$

Note that for  $s \rightarrow 0^+$  we obtain  $\mathcal{H}^2(p(J_u)) \geq 2h(4 - \sqrt{3})$  and for  $s \rightarrow 1^-$  we obtain  $\mathcal{H}^2(p(J_u)) \geq 2h$  (compare with (5.3)).  $\square$

## 6. A GENUS-TWO SURFACE THAT BEATS THE CONELIKE MINIMIZER

For a given  $h > 0$  and  $0 < s < 2 - \sqrt{3}$  we stick here with the choice of  $W$  (a solid elongated tetrahedron) given by Definition 2.2, i.e. with vertices having coordinates as in (2.1), see Figure 8, the regular tetrahedron corresponding to the choice  $h = \frac{\sqrt{2}}{2}$ .

Let us denote by  $\Sigma_c$  the usual conelike minimal surface spanning the one-skeleton of  $W$ , see Figures 1 left for a regular tetrahedron, and Figure 11 for an elongated tetrahedron. We shall compare  $\Sigma_c$  with a particular surface  $\Sigma$  corresponding to

FIGURE 8. Sketch of surface  $\Sigma$  with  $\tau = 2 - \sqrt{3}$  and  $h = 3$ .FIGURE 9. In grey the three components of  $\Sigma_v$ , vertical sections of  $\Sigma$  at  $x = -h\tau$  (left),  $x = 0$  (center),  $x = h\tau$  (right). The area of these grey regions is estimated from above by their convex envelopes (see (6.6)).

(i.e., being the projection of) the jump set of a *BV* function  $u$  in the domain of the functional  $\mathcal{F}$  (Theorem 6.2); the surface  $\Sigma$  will have genus two.

We shall show that there exists  $h > 1$  sufficiently large such that the area of  $\Sigma$  is less than the area of  $\Sigma_c$  (Theorem 6.1), giving quite strong evidence that  $\Sigma_c$  is not area-minimizing among minimal films if we allow for a more complex topology.

**6.1. Constructing the surface  $\Sigma$  using the covering space.** Let  $\tau \in (s, 1)$  be a parameter to be chosen later. The Lipschitz surface  $\Sigma$  is constructed by joining five pieces,

$$\Sigma = \Sigma_1 \cup \Sigma_2 \cup \Sigma_3 \cup \Sigma_4 \cup \Sigma_v, \quad (6.1)$$

four of which are defined each on sections of  $W$ , obtained by sectioning the wedge with the three planes  $\{x = 0\}$ ,  $\{x = \pm h\tau\}$ , see Figure 8, and the last one being “vertical”.

*Case  $x \in (-h, -h\tau)$  and  $x \in (h\tau, h)$ :* the surface  $\Sigma_i$ ,  $i \in \{1, 4\}$  is chosen coincident with  $\Sigma_c$ , more precisely  $\Sigma_1 := \Sigma_c \cap \{x < -h\tau\}$  and  $\Sigma_4 := \Sigma_c \cap \{x > h\tau\}$ .

*Case  $x \in (0, h\tau)$ :* the surface  $\Sigma_3$  coincides with the top and bottom faces of  $W$ .

*Case  $x \in (-h\tau, 0)$ :* the surface  $\Sigma_2$  coincides with the front and back faces of  $W$ .

In order to close the surface we need to add three “vertical” pieces, cumulatively denoted by  $\Sigma_v$  (see Figure 9), union of the square obtained by intersecting  $W$  with the vertical plane  $\{x = 0\}$  and of the parts of the two rectangles resulting as the intersection of  $W$  with the two planes  $\{x = \pm h\tau\}$ .

**Theorem 6.1.** *If  $\tau \in (s, 1)$  is small enough and  $h \in (1, +\infty)$  is large enough depending on  $\tau$ , we have*

$$\mathcal{H}^2(\Sigma) < \mathcal{H}^2(\Sigma_c). \quad (6.2)$$

*Proof.* We have to show that

$$\mathcal{H}^2(\Sigma_1) + \mathcal{H}^2(\Sigma_2) + \mathcal{H}^2(\Sigma_3) + \mathcal{H}^2(\Sigma_4) + \mathcal{H}^2(\Sigma_v) < \mathcal{H}^2(\Sigma_c), \quad (6.3)$$

provided  $\tau \in (s, 1)$  is small enough and  $h = h(\tau) \in (1, +\infty)$  is large enough.

In view of the definition of  $\Sigma$  we have

$$\mathcal{H}^2(\Sigma_c \cap \{|x| > h\tau\}) = \mathcal{H}^2(\Sigma \cap \{|x| > h\tau\}),$$

and therefore inequality (6.3) is equivalent to

$$\mathcal{H}^2(\Sigma_2) + \mathcal{H}^2(\Sigma_3) + \mathcal{H}^2(\Sigma_v) < \mathcal{H}^2(\Sigma_c \cap \{-h\tau < x < h\tau\}). \quad (6.4)$$

For  $t \in [0, 1]$  take the plane  $\pi_t = \{x = ht\}$ . Its intersection with the wedge  $W$  is a rectangle of sides  $1+t$  and  $1-t$ . Since  $\Sigma_c$  divides  $W$  into four disjoint solid regions, one per face, it follows that  $\Sigma_c \cap \pi_t$  divides the rectangle into four disjoint regions. Hence

$$\mathcal{H}^1(\Sigma_c \cap \pi_t) \geq 1 + \sqrt{3} - (\sqrt{3} - 1)t, \quad (6.5)$$

where the expression on the right hand side is the length of the Steiner tree joining the four vertices of the rectangle.

For a given  $\tau \in (s, 1)$  we shall need a bound from below of the section  $\Sigma_c \cap \{-h\tau < x < h\tau\}$ : using the generalized coarea formula [4, Theorem 3, pag. 103] and (6.5), we have

$$\begin{aligned} \mathcal{H}^2(\Sigma_c \cap \{-h\tau < x < h\tau\}) &\geq \int_{-h}^h \mathcal{H}^1(\Sigma_c \cap \{-h\tau < x < h\tau\} \cap \pi_t) dt \\ &\geq 2h \int_0^\tau (1 + \sqrt{3} - (\sqrt{3} - 1)t) dt \\ &= 2(1 + \sqrt{3})h\tau - (\sqrt{3} - 1)h\tau^2. \end{aligned}$$

Therefore, in order to show (6.4) it is sufficient to prove

$$\mathcal{H}^2(\Sigma_2) + \mathcal{H}^2(\Sigma_3) + \mathcal{H}^2(\Sigma_v) < 2(1 + \sqrt{3})h\tau - (\sqrt{3} - 1)h\tau^2.$$

Since all intersection rectangles have the same perimeter and the central square has area equal to one, we have

$$\mathcal{H}^2(\Sigma_v) \leq 3, \quad (6.6)$$

and so it will be sufficient to prove

$$\mathcal{H}^2(\Sigma_2) + \mathcal{H}^2(\Sigma_3) + 3 < 2(1 + \sqrt{3})h\tau - (\sqrt{3} - 1)h\tau^2. \quad (6.7)$$

Now, the area of the top (or bottom) facet  $F$  of  $W$  (the one having the vertex on the left and the basis on the right) equals  $\sqrt{4h^2 + 1}$ , therefore

$$\begin{aligned} \mathcal{H}^2(F \cap \{x < h\tau\}) &= \frac{(1 + \tau)^2}{4} \sqrt{4h^2 + 1}, \\ \mathcal{H}^2(F \cap \{0 < x < h\tau\}) &= \frac{(1 + \tau)^2}{4} \sqrt{4h^2 + 1} - \frac{1}{4} \sqrt{4h^2 + 1}. \end{aligned}$$

It follows

$$\mathcal{H}^2(\Sigma_2) + \mathcal{H}^2(\Sigma_3) = 4\mathcal{H}^2(F \cap \{0 < x < h\tau\}) = (2 + \tau)\tau\sqrt{4h^2 + 1},$$

so that (6.7) will be proved if we show

$$L := \frac{1}{h\tau} \left[ (2 + \tau)\tau\sqrt{4h^2 + 1} + 3 \right] < 2(1 + \sqrt{3}) - (\sqrt{3} - 1)\tau =: R.$$

Let us select  $\tau \in (s, 1)$  sufficiently small so that

$$4 + 2\tau < 2(1 + \sqrt{3}) - (\sqrt{3} - 1)\tau, \quad (6.8)$$

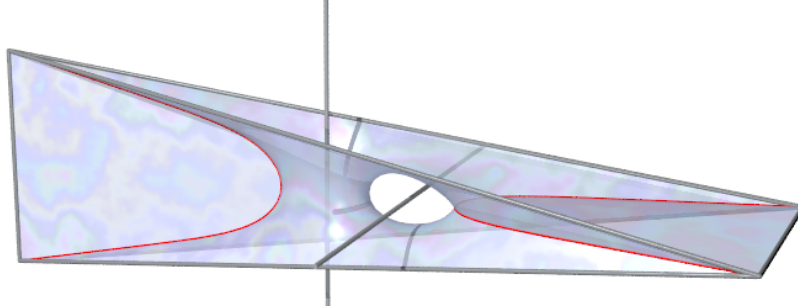


FIGURE 10. Minimal film obtained numerically starting a gradient flow from  $\Sigma$  with  $\tau = 2 - \sqrt{3}$  and  $h = 3.5$ . Computation performed with the **surf** software code by Emanuele Paolini.

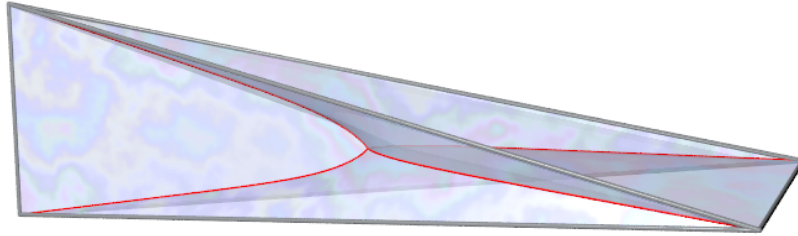


FIGURE 11. The conelike solution  $\Sigma_c$  with  $h = 3.5$ . Note that only the two lunette-surfaces are flat. Computation performed with the **surf** software code by Emanuele Paolini.

one possibility is e.g. to chose  $\tau = 2 - \sqrt{3}$ , consistent with  $\tau \in (s, 1)$  in view of the constraint on  $s$  imposed at the beginning of this section. Then we have

$$\lim_{h \rightarrow +\infty} L = (4 + 2\tau) < R,$$

and the result follows.  $\square$

Inequality (6.8) is solved for  $0 < \tau < 2(2 - \sqrt{3})$ . Values leading to inequality 6.2 are e.g.

$$\tau = 2 - \sqrt{3}, \quad h = 16,$$

they lead to the values

$$\mathcal{H}^2(\Sigma) \approx 22.456 + c, \quad \mathcal{H}^2(\Sigma_c) \approx 22.585 + c$$

where  $c$  is the common value

$$c := \mathcal{H}^2(\Sigma_c \cap \{|x| > h\tau\}) = \mathcal{H}^2(\Sigma \cap \{|x| > h\tau\}),$$

**Theorem 6.2.** *For any choice of  $s \in (0, 2 - \sqrt{3})$  select the base space  $M = M_{h,s}$  in Definition 2.2 with  $h$  large enough (e.g.  $h > 16$ ). Then there exists  $u \in D(\mathcal{F})$  such that its jump set projects exactly onto the surface  $\Sigma$  defined in (6.1), i.e.  $p(J_u) = \Sigma$ , and  $\mathcal{F}(u) = \mathcal{H}^2(\Sigma)$ . In particular*

$$\mathcal{F}_{\min}(M) < \mathcal{H}^2(\Sigma_c).$$

*Proof.* Fix  $\tau = 2 - \sqrt{3}$  and let  $\Sigma$  be the corresponding surface constructed above. Proving the result amounts to construct a function  $u : Y \rightarrow \{0, 1\}$  satisfying the required constraints to ensure  $u \in D(\mathcal{F})$  and with jump set  $J_u$  that projects onto

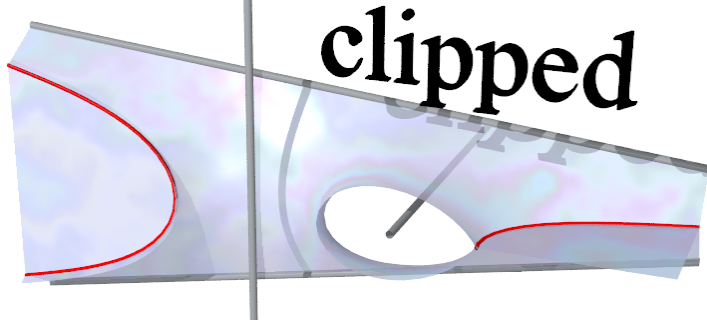


FIGURE 12. A zoom of the computed minimal surface of Figure 10 clipped at  $y = 0$ , the  $120^\circ$  condition can be clearly seen at the right hole.

$\Sigma$ . This can be done by first defining  $u(y) = 1$  (resp.  $= 0$ ) for  $p(y)$  outside  $W$  and in sheet 1 (resp. in sheets 2 and 3) and then extending it inside the tetrahedron by carefully making it jump when the projection crosses  $\Sigma$ . Since  $s < 2 - \sqrt{3} = \tau$ , it follows that the invisible wires do not intersect  $\Sigma$ , which in turn allows us to extend  $u$  as a constant in a neighborhood of  $C_{12}$  (compare Figure 6).  $\square$

Function  $u$  can also be constructed directly using the abstract definition of the covering (Section 4.2) as follows. First we need to fix an orientation and decide a permutation  $\sigma \in S_3$  for each smooth portion of  $\Sigma$ . This is done consistently to the permutations of Figure 6, for example we associate the permutation  $(1, 3, 2)$  to the left flat “lunette” when traversing it from front to back. We also need two “phantom” disks mimicking the cutting disks of figure 6 (with associated permutation  $(2, 3)$ ) that cut e.g. the frontal trapezium with a vertical line in a right part with permutation  $(1, 3, 2)$  and a left part with permutation  $(1, 2, 3)$  (when traversing it from front to back). The central vertical square would have the permutation  $(1, 3, 2)$  associated to it when traversing from right to left. In a similar fashion we attach a suitable permutation to all the remaining (oriented) portions of the surface, taking into account that the top trapezium is also divided in two parts by the phantom disk.

Now we first define a function  $\hat{u}$  on the set  $\hat{Y}$  of paths in  $M$  starting at the base point  $m_0$ . If  $\gamma$  is such a path with  $x := \gamma(1) \notin \Sigma$ , we can suppose, up to a small deformation in the same homotopy class, that it has only transversal intersections with  $\Sigma$  and no intersections with the triple curves nor with the intersection of the phantom disks with  $\Sigma$ . Then we can enumerate the permutations associated to the intersections of  $\gamma([0, 1])$  with  $\Sigma$  and the phantom disks or their inverse (based on whether  $\gamma$  traverses the surface in a positive or negative direction with respect to its selected orientation) and multiply all these permutations to obtain  $\sigma_\gamma \in S_3$ . If the final permutation fixes 1, i.e.  $\sigma_\gamma(1) = 1$ , then we define  $\hat{u}(\gamma) = 1$ , otherwise  $\hat{u}(\gamma) = 0$ .

The desired function  $u : Y \rightarrow 0, 1$  is now defined as  $u([\gamma]) = \hat{u}(\gamma)$  where  $[\gamma]$  is the equivalence class of all paths  $\eta \sim \gamma$  as defined in Section 4.2. It is now necessary to show that this is a good definition, in other words, that  $\hat{u}(\gamma_1) = \hat{u}(\gamma_2)$  whenever  $\gamma_1 \sim \gamma_2$ , i.e. whenever  $[\gamma_1 \gamma_2^{-1}] \in H$ . It is readily seen that this is a consequence of the stronger requirement that  $\hat{u}(\gamma) = 1$  for all  $\gamma$  closed loop with  $[\gamma] \in H$  which we now prove.

The choice of permutations on the pieces of surface is chosen such that the final permutation computed on a closed loop  $\gamma$  is insensitive to homotopic deformations of  $\gamma$ , so that we only need to show that  $\sigma_\gamma$  fixes 1 whenever  $[\gamma] \in H$ . This is true

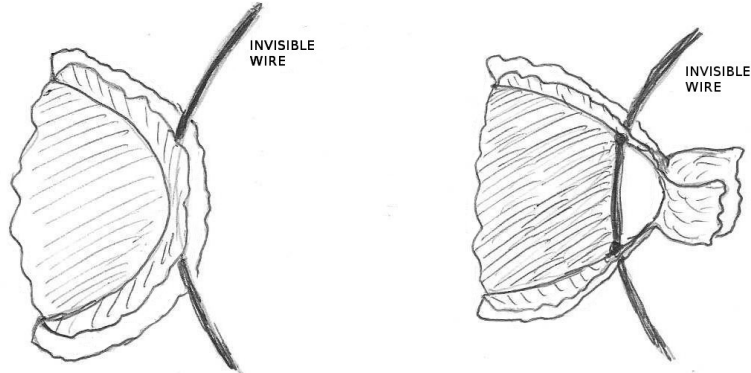


FIGURE 13. When the invisible wire approaches the triple curve (left) it becomes energetically convenient for the surface to jump into a configuration (right) where the invisible wire gets partially wetted (thus no longer invisible!) and a new hole is created right of the wire.

precisely because the choice of the permutations mimics the permutations used to define the covering by cut and paste displayed in Figure 6.

*Remark 6.1.* Inequality 6.2 is crucial in trying to actually prove the existence of a minimal film spanning an elongated tetrahedral frame with positive genus, since it shows the existence of a surface with the desired topology having area strictly less than the minimal area achievable with conelike surfaces. The candidate would be a minimizer of  $\mathcal{F}$ , since Theorem 6.2 implies that  $\mathcal{F}_{\min}(M) < \mathcal{H}^2(\Sigma_c)$ . However we still are unable to conclude, because we cannot exclude that the minimizing surface interferes with the invisible wires (see Section 7). Numerical simulations however strongly suggest that with appropriate choice of  $h$  and  $s$  in  $M_{h,s}$  this is not the case (Figure 10).

## 7. WHAT CAN GO WRONG?

For a fixed choice (sufficiently large) of  $h$  the minimum value  $\mathcal{F}_{\min}(M)$  will depend on the relative position of the invisible wires  $C_{12}$  with respect to the tetrahedral frame. Our first guess would be that for a wide range of positions (those for which  $C_{12}$  does not touch the minimizing surface) such value is constant, and so is a minimizer of the functional.

When  $C_{12}$  leaves such a set of positions we would expect the minimum value to increase a bit, since in that case the invisible wires impose a further constraint to the jump set of a minimizer. Indeed the wires would “push” on the surface and act as an obstacle for as long as the deformed surface bends at the wire with an angle larger than  $120^\circ$ .

Beyond the  $120^\circ$  threshold we expect one of the local “Taylor” rules [11] for a minimizing film to take effect and observe the formation of a new (fin-like) portion of the surface connecting a portion of  $C_{12}$ , let us call it the “wetted portion”, to a triple curve on the deformed surface meeting at angles of  $120^\circ$ .

The story is however completely different if  $C_{12}$  is moved to meet one or both of the two triple curves of the minimizing surface (red curves in Figure 10 ).

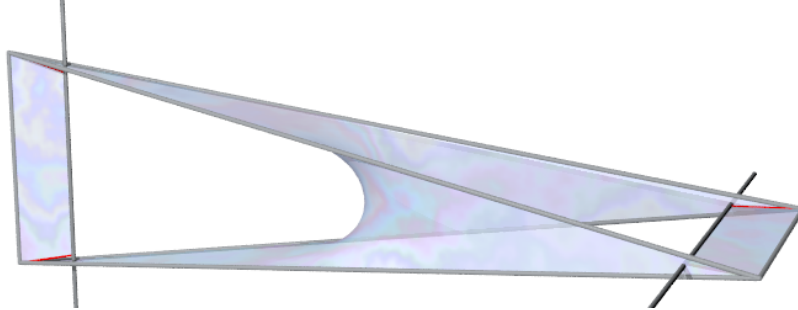


FIGURE 14. If the invisible wires approach the two short edges, the minimizer takes the structure shown in the picture ( $h = 3.5$ ). The invisible wires are partially wetted by the film. Four short triple curves join the vertices of the frame with the boundaries of the wetted portion of the invisible wires.

In this situation it is energetically favorable for the surface to suddenly jump into a configuration where a large portion of  $C_{12}$  is wetted by the flat part of the minimizer (Figure 13). Two new holes in the surface would then be created.

Actually this would be even more dramatic, since the formation of two smooth catenoid tunnels would come out in a situation where the tunnels are too long to be stable, so we also expect the tunnels to disappear completely with a final configuration resembling the one that would be obtained by a film that does not wet  $S_1$  and  $S_2$  with the addition of two flat trapezoid portions connecting e.g.  $S_1$  with part of  $C_1$  and with the rest of the surface (similarly on the right), see Figure 14.

In order to rule out this possible minimizer we can derive a lower bound for the surface area in such a configuration.

**Definition 7.1.** For a given choice of  $h > 0$  and  $0 < s < 1$  and selecting  $M = M_{h,s}$  we say that a surface  $\Sigma$  is “Steiner-like” if it satisfies properties (P1) and (P2) of Theorem 5.2 and moreover the intersection  $\Sigma \cap \pi_t$  with  $\pi_t = \{x = ht\}$  and  $|t| > s$  separates the four sides of the rectangle  $W \cap \pi_t$ .

**Theorem 7.1.** Let  $s < 2 - \sqrt{3}$ . A Steiner-like surface  $\Sigma_{\text{steiner}}$  can be modified into a surface  $\Sigma$  similar to the one constructed in Section 6.1 that does not wet the invisible wires and has lower area provided we chose  $s$  small enough and then  $h$  large enough. Consequently  $\Sigma_{\text{steiner}}$  cannot be a minimizer of functional  $\mathcal{F}$ .

*Proof.* The proof mimics that of Theorem 6.1, we modify  $\Sigma_{\text{steiner}}$  in the region  $-h\tau < x < h\tau$  with the choice  $\tau = 2 - \sqrt{3}$  exactly as we did for Theorem 6.1 obtaining a surface  $\Sigma$ . Using again the generalized coarea formula, the sectional estimate (5.4) with the second case also if  $|t| < 2 - \sqrt{3}$  and (5.5), we have

$$\begin{aligned} & \mathcal{H}^2(\Sigma_{\text{steiner}} \cap \{-h\tau < x < h\tau\}) \\ & \geq \int_{-h\tau}^{h\tau} \mathcal{H}^1(\Sigma \cap \pi_t) dt \\ & \geq 2h \int_0^s (2 - 2t) dt + 2h \int_s^{\tau} \left[ 1 + \sqrt{3} - (\sqrt{3} - 1)t \right] dt \\ & = h[(2 + 2\sqrt{3})\tau - (\sqrt{3} - 1)\tau^2 - (2\sqrt{3} - 2)s - (3 - \sqrt{3})s^2] \end{aligned}$$

that has to be compared with

$$\mathcal{H}^2(\Sigma \cap \{-h\tau \leq x \leq h\tau\}) = (2 + \tau)\tau\sqrt{4h^2 + 1} + 3$$

The only difference with the derivation of Theorem 6.1 is the presence of the two terms containing the parameter  $s$ . They however vanish as  $s \rightarrow 0$ , so that by selecting  $s$  sufficiently small we can again conclude if  $h$  is sufficiently large.  $\square$

## 8. ALL POSSIBLE COVERINGS

We want to describe all possible coverings of the base space  $M$  of degree 3 among those that will produce soap films that touch all six edges of the wedge and is not forced to touch the invisible circular wires. Here the fundamental group comes obviously into play, since we do that by describing all possible monodromy actions on the fiber above the base point  $m_0$ . This monodromy action can equivalently be described as the action defined by a subgroup of  $\pi_1(B)$  of index 3 by right multiplication.

*Remark 8.1.* The presence of triple points in the wireframe of the tetrahedron, together with the wetting condition (implying the existence of triple lines in the minimizing film) requires the presence of at least two distinct and nontrivial monodromy actions on the fiber at infinity, hence the covering has at least degree 3.

*Remark 8.2.* A degree 3 covering cannot allow for the standard minimizing film for the tetrahedron. This is due to the presence of the central quadruple point of the minimizing film. Indeed we shall see that all coverings satisfying the constraints will require a nontrivial monodromy action on the fiber when circling the invisible wires, making them an essential feature in the construction of the base space. Of course we could allow for more than two invisible wires.

Let  $H$  a subgroup of  $\pi_1(M)$  of index 3, and denote by  $s_1 := H$ ,  $s_2 := Hw_2$  and  $s_3 := Hw_3$  its right cosets, for some choice of representative elements  $w_2, w_3 \in \pi_1(M)$ . The elements of  $\pi_1(M)$  define an action on  $\{s_1, s_2, s_3\}$  defined by  $g : h \rightarrow hg$  (right multiplication by  $g \in \pi_1(B)$ ). If  $h', h''$  are in the same right coset then  $h'g(h''g)^{-1} = h'(h'')^{-1}$  and the definition is wellposed.

We then have a map  $\pi_1(M) \rightarrow S_3$  that to any element of  $\pi_1(M)$  associates an element of the permutation group of the three cosets. A permutation of  $S_3$  is interpreted as a permutation of the indices in  $\{s_1, s_2, s_3\}$ .

By composition, this map is defined once we know its value on the generators of  $\pi_1(M)$ .

In conclusion we have permutations  $\sigma_a, \sigma_b, \sigma_c, \sigma_d, \sigma_e \in S_3$  (permutations of  $\{1, 2, 3\}$ ) associated to the generators  $a, b, c, d, e$  respectively.

We now impose a number of constraints.

**Consistency with relators:** In the group presentation (3.2) the two relators must be consistent with the choice of the permutations  $\sigma_a, \dots, \sigma_e$ . In other words  $\sigma_a$  must commute with  $\sigma_b$  and  $\sigma_d$  must commute with  $\sigma_e$ . Take for example  $\sigma_a$  and  $\sigma_b$ ; they commute if and only if one of the following mutually exclusive conditions holds:

- (1)  $\sigma_a$  or  $\sigma_b$  is the identity permutation  $()$ ;
- (2)  $\sigma_a$  and  $\sigma_b$  are both cyclic of order 3, hence a power of  $(1, 2, 3)$ ;
- (3)  $\sigma_a = \sigma_b$  are the same transposition.

**Invisible-wire conditions:** The area-minimizing surface that we wish to model must not wet the two circular loops associated to generators  $a$  and  $e$  in Figure 3. In particular, a closed path starting at the base point in  $M$  and looping around one of such loops must not necessarily traverse the surface. Consequently the generators  $a$  and  $b$  must not move sheet 1 of the covering. The corresponding condition reads then as

$$\sigma_a, \sigma_e \in \{(), (2, 3)\}; \quad (8.1)$$

**Wetting conditions:** We want to reconstruct an area-minimizing surface that spans all six sides of the wedge. In other words, any tight loop around these edges should cross the surface. This condition is somewhat tricky to impose, particularly in situations where the covering is not normal, because we need to state our condition on elements of the  $\pi_1(M)$ , which requires to connect the base point to the tight loop. We end up with a condition that depends on *how* we choose the connecting path. Changing the path amounts to performing a conjugation on the element of  $\pi_1(M)$ . A strong wetting condition could be that any element in  $\pi_1(M)$  that loops once around the selected edge must move all sheets (the permutation is required to be a derangement). This condition is insensitive to conjugation. A weaker condition is to require that the element of  $\pi_1(M)$  moves sheet 1 (the sheet where  $u = 1$  at the base point  $m_0$ , far from  $W$ ). This condition however depends on how we connect the tight loop to the base point. It seems only natural to require the connecting path to lie outside the wedge, which is not the same as requiring the corresponding Wirtinger-type loop in the diagram of Figure 3 to move sheet 1. In particular this is not true for  $L_3$  the long edge that in Figure 3 runs in the back and does not cross the two disks, for which a linking path that does not enter the wedge is  $bc^{-1}$ . In the end the wetting conditions read as:

$$\begin{aligned} \sigma_c, \quad \sigma_c^{-1}\sigma_d, \quad \sigma_b\sigma_c^{-1}, \quad \sigma_b\sigma_c^{-1}\sigma_d, \\ \sigma_a\sigma_d^{-1}\sigma_c\sigma_a^{-1}\sigma_c^{-1}, \quad \sigma_b\sigma_c^{-1}\sigma_e\sigma_c\sigma_e^{-1} \notin \{(), (2, 3)\} \end{aligned} \quad (8.2)$$

The third relation comes from  $\sigma(L_{4,2})^{-1}\sigma(L_{3,3})\sigma(L_{4,2})$ , where  $\sigma(L_{i,j})$  is the permutation associated to the varius long edges in (3.1), after substitution and simplification. It corresponds to a path that, as mentioned above, starts at  $m_0$ , runs in the back of  $L_4$  from below, than around  $L_3$ , than again in the back of  $L_4$  and back to  $m_0$ . The fourth relation is the inverse of  $\sigma(L_{4,2})$ .

We shall now search for all possible choices of  $\sigma_a$  through  $\sigma_e$  that are compatible with the three set of constraints (8.1), (8.2) and consistency with the relators of the presentation.

*Remark 8.3.* Our search also includes the special cases were one or both of the invisible wires  $C_1$  and  $C_2$  are not present, since the choice, say,  $\sigma_a = ()$  (the identity permutation) leads to the same result as removal of  $C_1$ .

We separately analize the possibilities with all possible choices of  $\sigma_a$  and  $\sigma_e$  allowed by (8.1) arriving to the conclusion that the presence of both invisible wires is essential.

**8.1. Searching coverings for  $\sigma_a = \sigma_e = ()$ .** First note that all constraints above are insensitive to exchange of sheets 2, and 3. This means that for definiteness we can assume that  $\sigma_c(1) = 2$ , which in view of the first wetting constraint in (8.2) leaves us with only two possibilities:  $\sigma_c = (1, 2)$  or  $\sigma_c = (1, 2, 3)$ .

**8.1.1. Case  $\sigma_c = (1, 2, 3)$ .** Wetting constraints 2, 3, 5, 6 imply  $\sigma_d \in \{(1, 3, 2), (1, 2)\}$  resulting in  $\sigma_c^{-1}\sigma_d$  sending  $3 \mapsto 1$ . Moreover  $\sigma_b \in \{(1, 3, 2), (1, 3)\}$  resulting in  $\sigma_b$  sending  $1 \mapsto 3$ . This would imply  $\sigma_b\sigma_c^{-1}\sigma_d$  sending  $1 \mapsto 1$ , contrary to wetting constraint 4.

**8.1.2. Case  $\sigma_c = (1, 2)$ .** Wetting constraints 2, 3, 5, 6 imply  $\sigma_d \in \{(1, 2, 3), (1, 3)\}$  resulting in  $\sigma_c^{-1}\sigma_d$  sending  $3 \mapsto 1$ . Moreover  $\sigma_b \in \{(1, 3, 2), (1, 3)\}$  resulting in  $\sigma_b$  sending  $1 \mapsto 3$ . This would imply  $\sigma_b\sigma_c^{-1}\sigma_d$  sending  $1 \mapsto 1$ , contrary to wetting constraint 4.

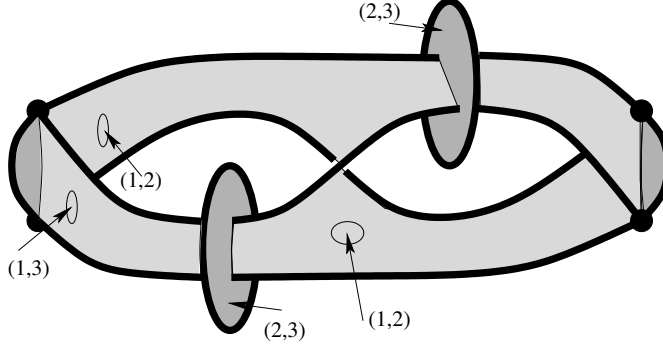


FIGURE 15. An alternative covering definition that should lead to the same minimizing film for the covering of Figure 6.

8.2. **Searching coverings for  $\sigma_a = ()$  and  $\sigma_e = (2, 3)$ .** Again we can assume that  $\sigma_c(1) = 2$ .

Reasoning as before, from  $\sigma_a = ()$  we get  $\sigma_d \in \{(1, 3, 2), (1, 2, 3), (1, 2), (1, 3)\}$ . However  $\sigma_d$  and  $\sigma_e$  must commute, which is incompatible with  $\sigma_e = (2, 3)$ .

8.3. **Searching coverings for  $\sigma_a = (2, 3)$  and  $\sigma_e = ()$ .** Again we can assume that  $\sigma_c(1) = 2$ .

Reasoning as before from  $\sigma_e = ()$  we get  $\sigma_b \in \{(1, 3, 2), (1, 2, 3), (1, 2), (1, 3)\}$ , which does not commute with  $\sigma_a$ .

8.4. **Searching coverings for  $\sigma_a = \sigma_e = (2, 3)$ .** Consistency with the relators of the group presentation leads to

$$\sigma_b, \sigma_d \in \{(), (2, 3)\}, \quad \sigma_c \notin \{(), (2, 3)\}.$$

A direct check shows that any choice satisfying the requirements above also satisfies all constraints for our covering.

Figure 15 shows the covering that corresponds to the choice

$$\sigma_b = \sigma_d = (), \quad \sigma_c = (1, 2).$$

The resulting covering is clearly not isomorphic to the one constructed in Section 4 and it is a natural question whether the minimization problem  $\mathcal{F}(u) \rightarrow \min$  in this context leads to the same result. This is entirely possible but we did not pursue the subject.

On the other hand we actually can find functions  $u \in D(\mathcal{F})$  (with  $D(\mathcal{F})$  redefined based on the new covering) with a jump set that is incompatible with the former definition of  $D(\mathcal{F})$ . We can construct such function by making it jump across a big sphere that encloses  $W$  with the sheet where its value is 1 that changes from 1 to 3. Then it is possible to take advantage of the fact that the wetting conditions are weak and with  $u = 1$  on sheet 3 they do not impose wetting of e.g.  $L_{1,1}$  resulting in the possibility (actually achievable) of an only partially wetted  $L_1$ . Similarly for the other long edges.

Clearly, however, such a surface cannot be a minimizer.

## 9. NUMERICAL SIMULATIONS AND CONCLUSIONS

A number of numerical simulations have been performed using the software code **surf** of Emanuele Paolini. It is based on a gradient flow with artificial viscosity starting from a triangulated surface having the required topology. It does not use the setting based on coverings of the present paper, however it gives a consistent result provided the starting surface is the set  $p(J_u)$  of some  $u \in D(\mathcal{F})$ , that there

is no change of topology and there is no touching of the invisible wires (they are not modelled by `surf`). Figures 7, 10, 11 have all been obtained by starting from suitable faceted initial surfaces, with the geometry corresponding to the choice  $h = 3.5$ , for example the result shown in Figure 10 is obtained by starting from the faceted surface displayed in Figure 8.

Numerically it turns out that with  $h = 3.5$  the area of the genus-two minimizer is slightly greater than the area of the conelike minimal surface; on the contrary increasing  $h$  to (e.g.)  $h = 4$  results in a genus-two surface that numerically beats the conelike minimizer, consistent with the results of Section 6.

Decreasing  $h$  changes the minimizing evolution drastically: after a (large) number of gradient flow iterations, the surface loses its symmetry (due to roundoff errors that break the symmetry of the problem) and one of the two holes shrinks at the expense of the other. The numerical evolution stops when the smaller hole completely closes, since the software cannot cope with changes of topology. Evolution after such singularization time depends on how the topology is modified. However it should be noted that the evolution would in this case typically impact with one of the invisible wires before the singularization time.

It is conceivable that for this value of  $h$  the evolution would produce a stationary surfaces, that is minimal among surfaces that are forced to have the same symmetries of the boundary frame.

Decreasing  $h$  even further, in particular taking the value that results in a regular tetrahedron, numerically produces an evolution where the two holes both shrink more or less selfsimilarly, so that we expect in the limit to obtain the conelike minimizer.

## REFERENCES

- [1] S. Amato, G. Bellettini, M. Paolini: *Constrained BV functions on covering spaces for minimal networks and Plateau's type problems*, Adv. Calc. Var. **4** (2015), 1–23.
- [2] L. Ambrosio, N. Fusco, and D. Pallara, *Functions of Bounded Variation and Free Discontinuity Problems*, Oxford Math. Monogr., Oxford, 2000.
- [3] K. Brakke, *Soap films and covering spaces*, J. Geom. Anal. **5** (1995), 445–514.
- [4] M. Giaquinta, G. Modica, J. Soucek, *Cartesian Currents in the Calculus of Variations I*, volume 37 *Ergebnisse der Mathematik und ihrer Grenzgebiete*, Springer-Verlag, Berlin Heidelberg 1998.
- [5] A. Hatcher, *Algebraic Topology*, Cambridge University Press, 2002.
- [6] R. Huff, *Conelike soap films spanning tetrahedra*, Trans. Amer. Math. Soc. **362** (2010), 5063–5081.
- [7] R. Huff, *An immersed soap film of genus one*, Comm. Anal. Geom. **19** (2011), 601–631.
- [8] G. Lawlor, F. Morgan, *Paired calibrations applied to soap films, immiscible fluids, and surfaces or networks minimizing other norms*, Pacific J. Math. **166** (1994), 55–83.
- [9] W. Magnus, A. Karrass, D. Solitar, *Combinatorial Group Theory: Presentations of Groups in Terms of Generators and Relations*, Dover Publications, 1976.
- [10] F. Morgan, *Geometric Measure Theory: A Beginners Guide*, Elsevier Science, 2008.
- [11] J. Taylor, *The structure of singularities in soap-bubble-like and soap-film-like minimal surfaces*, Ann. Math., **103** (1976), 489–539.